Spread Spectrum Modulation for LCL Filter Design

Ki-Bum Park
Power Electronics Department
ABB Corporate Research
Baden-Daettwil, Switzerland
ki-bum.park@ch.abb.com

Pascal Klaus
Electrical Engineering
EPFL
Laussane, Switzerland
pascal.klaus@epfl.ch

Ralph M. Burkart
Power Electronics Department
ABB Corporate Research
Baden-Daettwil, Switzerland
ralph.burkart@ch.abb.com

***Abstract*—The LCL filter is often the bulkiest component in grid-tied converters, which is designed to satisfy the grid harmonic standards such as IEEE519. To reduce the filter requirement, application of the spread spectrum modulation (SSM) to LCL filter design is investigated in this paper. Filter design methodology for SSM is presented and a comparative analysis between the conventional pulse-width modulation (PWM) and SSM is carried out focusing on their impact on the filter design. It is shown that under the same average switching frequency, LCL filter parameters required for SSM can be substantially reduced compared to the conventional PWM.**

Keywords—Pulse width modulation, spread spectrum modulation, LCL filter, random.

I. Introduction

Due to the significant growth of renewable generation such as photovoltaic and wind power, the number of installed grid-tied power electronic converters shown in **Fig. 1(a)** is increasing fast. The main objective of a grid-tied converter is providing a stable power flow between the loads/generators and the grid while satisfying the grid codes, in particularly harmonic current standards such as IEEE519 shown in **Fig. 1(b)** or BDEW [1],[2]. In order to mitigate the harmonic currents generated by the typically employed pulse-width modulated (PWM) voltage source converters (VSC), LCL filters have been widely used. Usually the LCL filter is the bulkiest and heaviest component in high power converters. In the case of a multi-megawatt system, the weight of the LCL filter can reach hundreds of kilograms.

Core technologies of grid-tied converters can be categorized from LCL filter design perspective, i.e., harmonic source and physical filter design [2]. Harmonic sources can be improved by increasing a carrier frequency, applying multilevel topology [3], interleaving topologies [4], or utilizing different modulation schemes [1],[16]. Among others, improving the harmonic spectrum by means of utilizing advanced modulation schemes is particularly attractive to high power system, since it can be applied without further development of high power hardware which requires significant time and resources. Conventional fixed frequency PWM shown in **Fig. 2(a)** generates high peak amplitude in harmonic spectrum, which requires significant attenuation of the LCL filter. Therefore, minimizing the highest harmonic components is a particularly effective approach when it comes to LCL filter design.

Spread spectrum modulation (SSM) as shown in **Fig. 2(b)** has been adopted for low power electronics to reduce EMI [5]-[7] and motor drive application to suppress audible noise [8]-[12]. To reduce the filter requirement, the application of SSM to grid-tied converters is investigated in this paper. The LCL filter design methodology for SSM is presented and a comparative analysis between the conventional PWM and SSM is carried out focusing on their impacts on the LCL filter design.

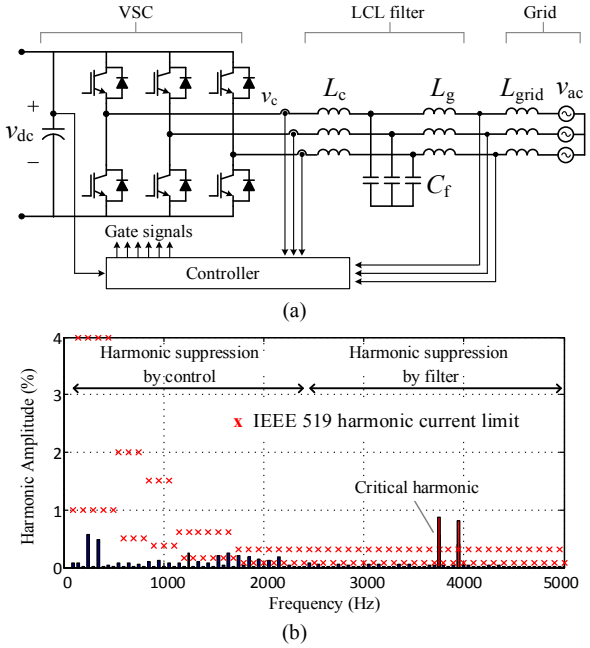

Fig. 1. (a) Grid-tied converter with LCL filter. (b) IEEE519 harmonic current standard and typical harmonic spectrum based on a conventional fixed frequency PWM.

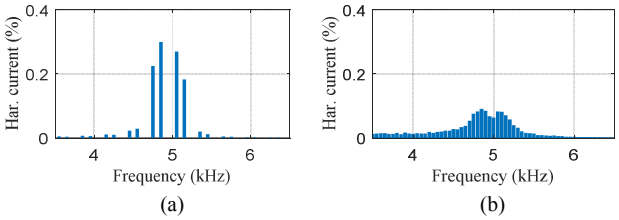

Fig. 2. Harmonic current spectrum comparison between (a) conventional PWM and (b) spread spectrum modulation when the same LCL filter is used.

II. Generalization of Spread Spectrum Modulation

The main objective of PWM is generating pulses of which the average value in a switching cycle follows the reference voltage. As presented in **Fig. 3**, in general, implementation of three-phase PWM can be broken down into the following three steps:

Step 1. Common-mode (CM) voltage injection
Step 2. Switching period selection
Step 3. Pulse positioning

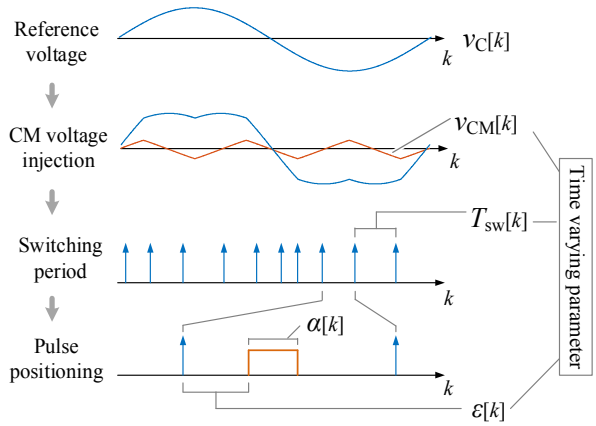

Fig. 3. Framework of PWM: common mode voltage injection → switching period selection → pulse positioning inside one switching period.

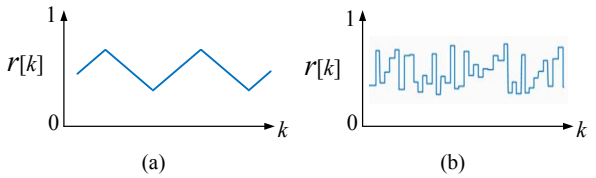

Fig. 4. Shape of time varying parameters, v_{CM}, T_{sw} or ε, to achieve a spread spectrum. (a) Periodic. (b) Randomized.

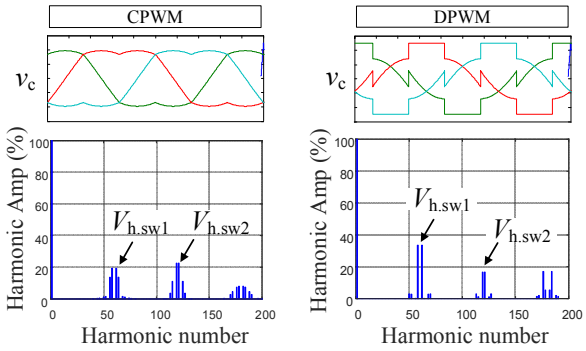

Fig. 5. Impact of injected common-mode voltage on harmonic spectrum of differential mode voltage.

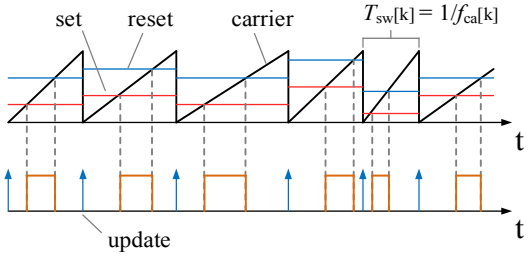

Fig. 6. Implementation of varying switching periods and pulse positionings using a sawtooth carrier and set/reset references.

Each of these steps affects the harmonic spectrum of PWM. When the operation of each step has fixed parameters, it results in harmonic spectrums where the harmonic components are concentrated in narrow frequency ranges as shown in **Fig. 2(a)**. On the other hand, by introducing the time varying parameters to any of these steps, the spreading effects of the harmonics can be achieved which results in lower peak harmonics as presented in **Fig. 2(b)**. In other words, common mode (CM) voltage $v_{CM}[k]$, switching period $T_{sw}[k]$, and pulse displacement $\varepsilon[k]$ can be a function of the time varying parameter $r[k]$, where k is number of switching period.

$$v_{CM}[k] = f_{CM}(r[k]) \ , \tag{1a}$$

$$T_{SW}[k] = f_{SW}(r[k]) \ , \tag{1b}$$

$$\varepsilon[k] = f_{E}(r[k]) \ . \tag{1c}$$

Any shape of time varying parameter can be used. Typically, two types of time varying parameters, as shown in **Fig. 4**, are popular for SSM:

- *Randomized*
- *Periodic*

The *Randomized* time variation is known for the best harmonic spreading effect for the given parameter variation range while the *Periodic* time variation is easy to implement in practice. Usually, sinusoidal or triangular shapes are used for the *Periodic* method [6]. The impact of the time-varying parameters in each step 1-3 on the harmonic spectrum is presented next.

A. Common-Mode Voltage Injection

In three-phase three-wire systems, the CM voltage is added to the original reference voltage of the PWM to increase the modulation index range, *Mi*. Although the CM voltage does not affect the fundamental components of the differential mode (DM) voltage of the three phase system, the harmonic spectrum of the DM voltage and CM voltage is changed according to the shape of the CM voltage, i.e., v_{CM}. **Fig. 5** shows the impact of v_{CM} on the harmonic spectrum. Usually, PWM with triangular-shape v_{CM}, also known as space vector modulation (SVM) or the continuous PWM (CPWM), provide good harmonic spectra while the discontinuous PWM (DPWM) produces higher harmonic contents at the cost of reduced switching losses [1]. CPWM or DPWM can be considered as specific examples of *Periodic* time varying parameter selection for v_{CM}. Since the main objective of CM voltage injection is the extension of *Mi*, CPWM is selected for the sake of analysis in the rest of the paper.

B. Switching Period Selection

The carrier frequency f_{ca} (=$1/T_{sw}$), or equivalently the switching period has the most significant influence on the harmonic spectrum. For a fixed f_{ca}, the harmonic spectrum appears around the selected carrier frequency. By introducing a time-varying carrier frequency, the harmonic spectrum also varies, i.e., the spectrum is spread over the frequency range of the time-varying carrier frequency as shown in **Fig. 6** [8]. Consequently, the wider f_{ca} varies, the wider the spectrum becomes. It is noted that both the *Periodic* or *Randomized* method can be used for f_{ca} variation. For the given minimum and maximum f_{ca}, the *Randomized* method results in the smallest harmonic peak amplitudes.

C. Pulse Positioning

Once T_{sw} is selected, the pulse can be positioned anywhere inside one switching period as far as the duty cycle does not change [9]-[11]. As shown in **Fig. 6**, arbitrary pulse positioning within the switching cycle can be implemented with a sawtooth carrier and set/reset comparator signals [10]. In three-phase systems, extensive research has been carried

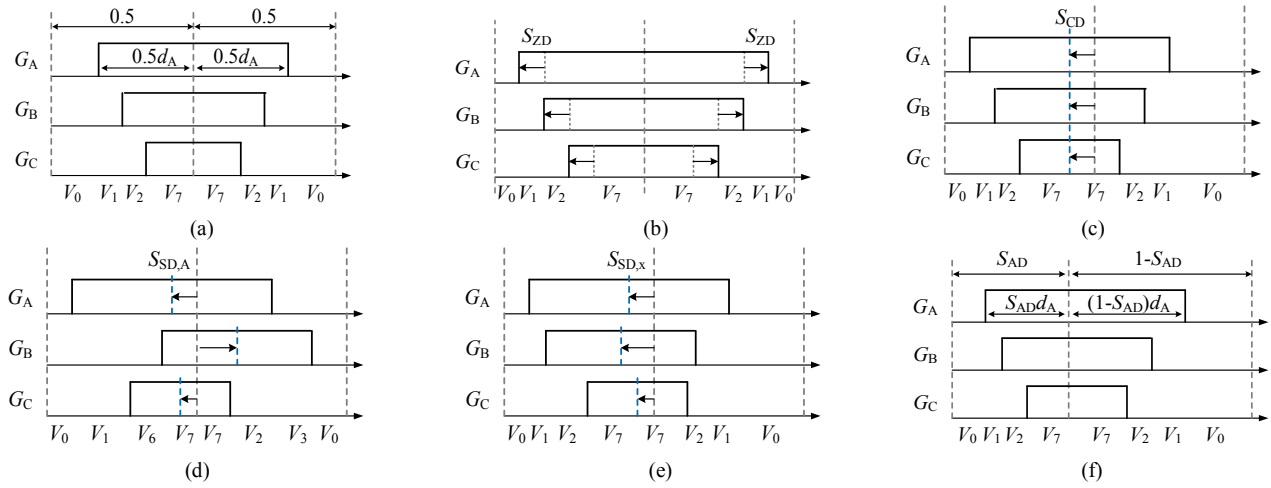

Fig. 7. Pulse positioning variation in one switching cycle for a three-phase system. (a) Conventional. (b) Zero vector distribution (ZD). (c) Center displacement (CD). (d) Separate displacement (SD). (e) Separate displacement with order (SO). (f) Asymmetric distribution (AD). $V_0 - V_7$ are space vectors defined in [16]

out under the topic of random PWM (RPWM) in motor drive applications [7]-[12]. Several different pulse positioning strategies for three-phase systems are available that differ with respect as shown in **Fig. 7**.

1) Zero Vector Distribution (ZD) : The ratio between the zero vectors (000/111) is varied every switching cycle while maintaining the total zero vector duration constant as shown in **Fig. 7(b)**. S_{ZD} is amount of extension or reduction of all pulses, which is a time varying parameter and can be expressed as (2). Here, '*r*' is an internal time varying parameter which can be either *Periodic* or *Randomized*, ranging from 0 to 1. Positive and negative sign of S_{ZD} means extension and reduction of pulses, respectively.

$$S_{ZD} = r(1-d_{max}) - (1-r)d_{min} \quad (2)$$

Note that this pulse positioning strategy is equivalent to varying the injected CM voltage v_{CM} (Section II-*A*) whose effect is also the variation of the ratio between the zero vectors.

2) Center Displacement (CD): The centers of all pulses in the three phases are shifted with the same amount as shown in **Fig. 7(c)**. The displacement duty cycle is expressed in (3). The maximum displacement is limited by the phase with the maximum duty cycle.

$$S_{CD} = (2r-1)(1-d_{max}) \quad (3)$$

3) Separate Displacement (SD): The position of each pulse is varied individually as shown in **Fig. 7(d)**. The original set and sequence of space vectors is not necessarily maintained. This leads to an arbitrary combination of space vectors to obtain the target voltage vector and eventually results in a higher current ripple.

$$S_{SD,x} = (2r-1)(1-d_x) \quad (4)$$

4) Separate Displacement with Order (SO): It is also possible to keep the order of space vector change with constraints on $S_{SD,x}$ as shown in **Fig. 7 (e)**.

5) Asymmetric Distribution (AD): The carrier is rendered asymmetric, i.e. the ratio of positive slope and negative slope of the carrier is varied in every switching cycle as shown in **Fig. 7(f)**. Random leading-lagging modulation in [9] can also be considered as an extreme asymmetric carrier operation.

$$S_{AD} = r \quad (5)$$

Variation of the spreading parameter $S = \{S_{ZD}, S_{CD}, S_{SD}, S_{SO}, S_{AD}\}$ is determined by the variation range of *r*, which is another design freedom for SSM. Both *Randomized* and *Periodic r* can be used. Once the spreading parameter *S* is determined, it is converted to the set/reset comparator timing as shown in **Fig. 6**. It should be noted that in addition to the above mentioned SSMs other types of SSM are also available [9],[10].

D. Comparison of Spread Spectrum Modulations

The impact of different pulse positionings and variable f_{ca} on the DM voltage harmonic spectrum is shown in **Fig. 8**. A *Randomized* time-varying parameter *r* is used for all cases. The impact of the pulse positioning under the same f_{ca} of 5 kHz is shown in **Fig. 8(a) - 8(f)**. When it comes to ZD and CD pulse positioning methods, the reduction of the peak harmonic voltage is negligible since they only affect the zero vector distribution that is already optimized in the benchmark CPWM. On the other hand, the SD, SO, and AD pulse positioning methods provide 2 to 3 times lower peak harmonic voltage (also depending on the modulation index *Mi*) since the active vector distribution is also affected. **Fig. 8(g)** shows the case with random variation of f_{ca}, which provides very effective harmonic spectrum spreading. The wider T_{sw} varies, the lower the peak harmonic voltage becomes. By combining the pulse positioning and variable f_{ca}, even wider spectrum spreading can be achieved as shown in **Fig. 8(h)**.

III. LCL Filter Design with Spread Spectrum Modulation

A. IEEE519 Harmonic Measurement

When it comes to SSM, harmonic spectrum can vary every fundamental cycle depending on the choice of time varying parameters. Therefore, the determined harmonic spectrum can also change depending on measurement method and procedure. IEEE519 standard specifies the harmonic spectrum to be obtained on the basis of *individual measurements* with a

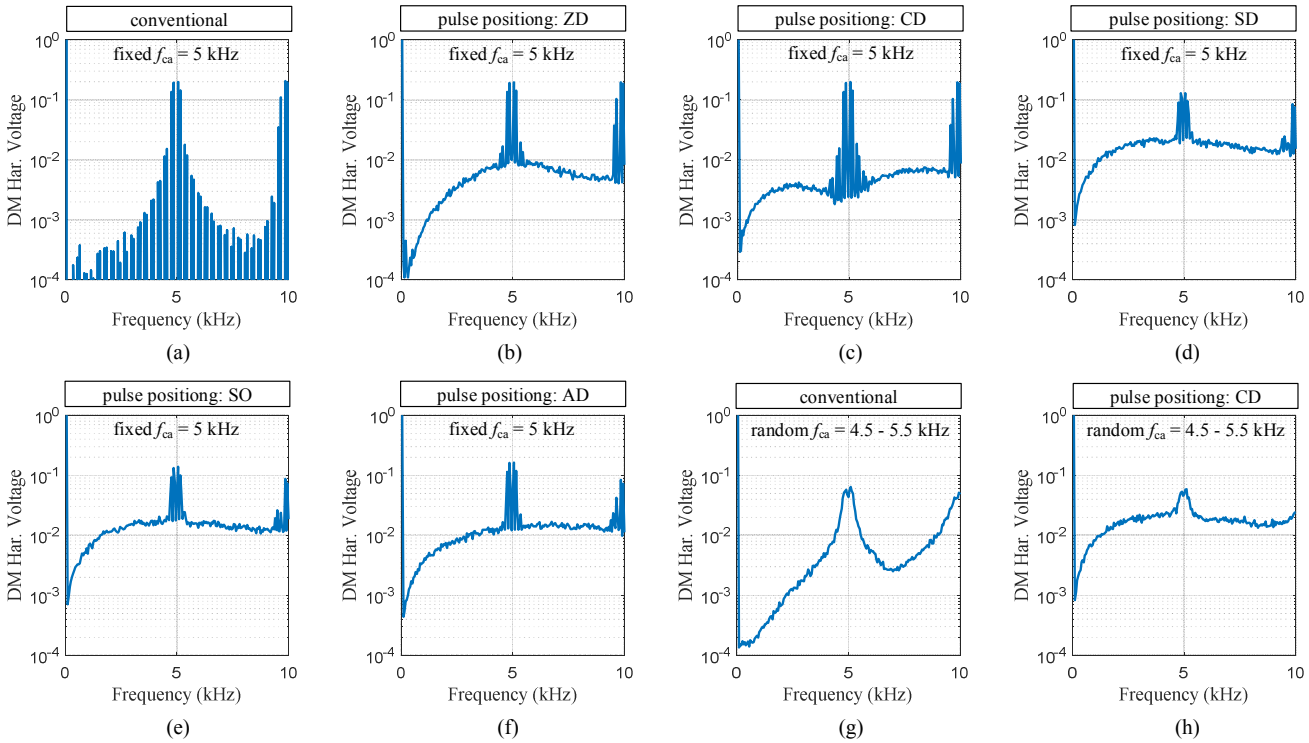

Fig. 8. Comparison of DM voltage harmonic spectrums of various SSM (b)-(h) against the conventional CPWM (a) for a modulation index *Mi*=1. The harmonics are normalized by the fundamental component.

window of 200-ms duration (10 cycles of 50 Hz system). The corresponding Fourier transform has a frequency resolution of 5 Hz. Furthermore, the standard specifies a harmonic magnitude to be the value at a center frequency combined with the two adjacent 5-Hz bin values. That is, three values are combined into a single RMS value that defines the harmonic magnitude for the particular center frequency component. The harmonic component from *individual measurements*, $F_{n,i}$, can be expressed as (6), where F_p is the magnitude (peak value) of an individual bin and k_n is the index of the bin corresponding to the *n*-th harmonic [14].

$$F_{n,i} = \sqrt{\sum_{k=k_n-1}^{k_n+1} \frac{F_P^2(k)}{2}} \tag{6}$$

According to the standard, the *very short time harmonic measurement* is based on the RMS combination of 15 *individual measurements*. The harmonic component of *very short time harmonic measurements*, $F_{n,vs}$, is expressed as (7)

$$F_{n,vs} = \sqrt{\frac{1}{15}\sum_{i=1}^{15} F_{n,i}^2} \tag{7}$$

B. Filter Design Methodology for SSM

The LCL filter is designed to satisfy the standard with a given harmonic voltage spectrum generated by the converter. The main challenge of designing a filter with SSM is that identifying the most significant harmonic voltage which produce the most significant harmonic current is more difficult compared to conventional PWMs since the harmonic spectrum is not well defined. The fundamental idea behind the filter design procedure for SSM is as follows: the resonance frequency ω_{res} of the filter represents a design variable that is selected by the user. Once it is selected, the shape of the frequency response of the filter is fixed. Equations (8) and (9)

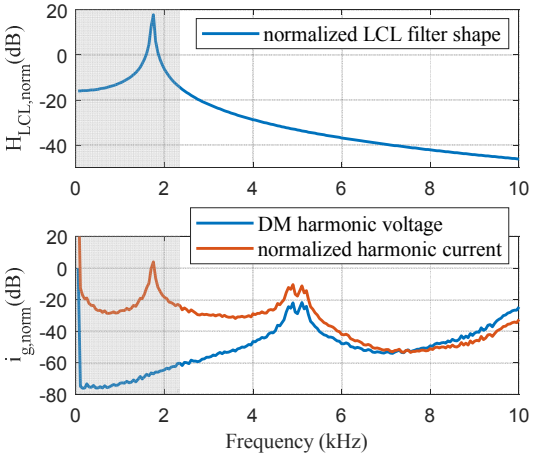

Fig. 9. LCL filter design. (a) Normalized LCL filter shape. (b) DM harmonic voltage and the corresponding normalized harmonic current. For the filter design, the highest normalized current harmonic is relevant where it is assumed that harmonics up to 1.3 times the resonance frequency are attenuated by active and passive damping schemes and the controller.

describe the transfer function of the LCL filter and its normalized form which only depends on ω_{res}.

$$\left|H_{LCL}(\omega)\right| = \frac{\omega_{res}^2}{(L_c + L_g)\omega\left|\omega_{res}^2 - \omega^2\right|} \tag{8}$$

$$\left|H_{LCL,norm}(\omega)\right| = \frac{\omega_{res}^2}{\omega\left|\omega_{res}^2 - \omega^2\right|} \tag{9}$$

Then, the total filter inductance (L_c + L_g) acts as a simple scaling factor between H_{LCL} and $H_{LCL,norm}$. The design procedure therefore first calculates the DM voltage generated

TABLE I. DESIGN SPECIFICATIONS

Input voltage v_{ac} (V_{rms})	690 line-to-line
Fundamental frequency (Hz)	50
DClink voltage v_{dc} (V)	1100
Output power P_{out} (MW)	1
Base inductor (mH)	1.5
Base capacitor (mF)	6.7

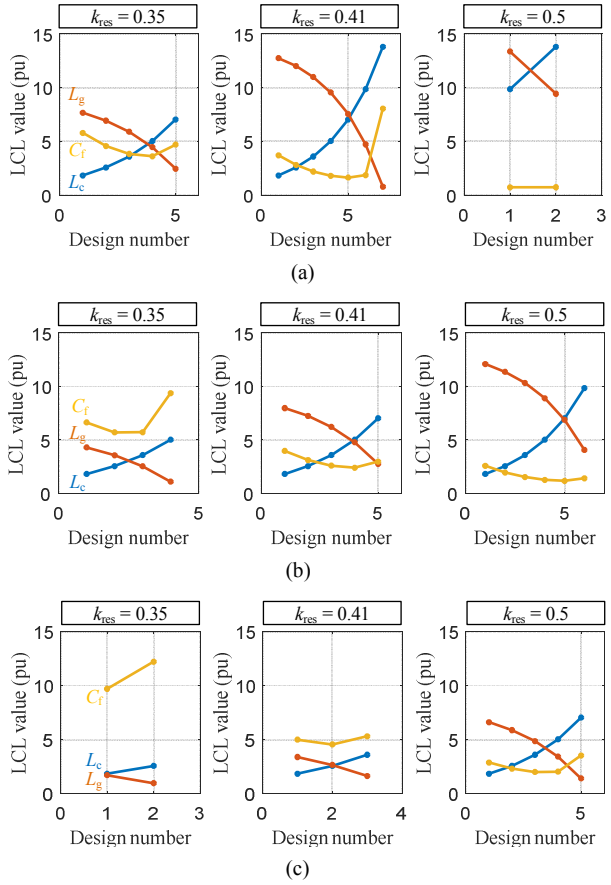

Fig. 10. Comparison of LCL filter parameter values (% p.u.) for (a) fixed f_{ca} = 5 kHz, (b) random f_{ca} = 4.8 – 5.2 kHz, and (c) random f_{ca} = 4.6 – 5.4 kHz. Conventional pulse positioning is used for all cases. k_{res} is the ratio between the filter resonant frequency and the average f_{ca}.

by PWM and takes its Fourier-transform and multiplies it with a $H_{LCL,norm}$ as can be seen in **Fig. 9**. The normalized harmonic current corresponds to the harmonic spectrum with a normalized filter with total inductance of 1 H and can be used to detect the most significant harmonic frequency. Note that it is assumed that harmonics up to 1.3 times the resonance frequency are sufficiently attenuated by passive and active damping schemes and the controller. Once the most significant harmonic frequency is determined, the total required filter inductance can be obtained to satisfy the standard. Considering IEEE519 measurement procedure given in (6) and (7), the most significant harmonic current, $I_{max,vs}$ can be expressed as (10), where k_{max} is the harmonic number for the most significant harmonic and $V_{p,i}$ is the peak DM harmonic voltage generated by the converter This must be smaller than the current limit specified by the standard, $I^*_{IEEE519}$. Once the converter side inductor L_c is selected, the remaining filter parameter L_g and C_f can be determined by (11) and (12), where *SM* is a design safety margin (%). It is noted that the same procedure can also be applied to other types of

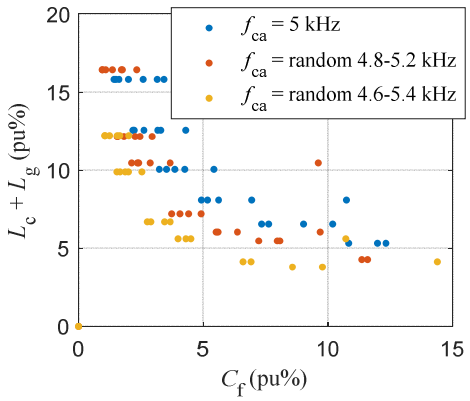

Fig. 11. Pareto comparison of LCL parameters between (a) fixed f_{ca} = 5 kHz, (b) random f_{ca} = 4.8 – 5.2 kHz, and (c) random f_{ca} = 4.6 – 5.4 kHz shown in Fig. 10.

filter design such as LLCL filter [15].

$$I_{\max,vs} = \frac{1}{(L_c + L_g)} \underbrace{\sqrt{\frac{1}{15}\sum_{i=1}^{15}\sum_{k=k_{\max}-1}^{k_{\max}+1} \frac{V_{P,i}^2(k)\left|H_{LCL,norm}^2(k)\right|}{2}}}_{I_{\max,vs,norm}} \quad (10)$$

$$L_g = \frac{I_{\max,vs,norm}}{I^*_{IEEE519}}\left(1 + \frac{SM}{100}\right) - L_c \quad (11)$$

$$C_f = \frac{L_c + L_g}{L_c L_g \omega_{res}^2} \quad (12)$$

IV. IMPACT OF SPREAD SPECTRUM MODULATION

A. LCL Filter Parameters

Based on the design procedure in the previous section, numerous combinations of LCL filter parameters can be generated. **Fig. 10** shows the impact of random variation of f_{ca} on the filter parameters with the design specifications of **Table I**. The x-axis represents different combinations of parameters and the y-axis shows the per unit values of the corresponding filter parameters. It is apparent that the required filter parameters become lower as the variation range of f_{ca} increases. **Fig. 11** shows the Pareto comparison of the filter parameters shown in **Fig. 10**. When the same filter capacitance is used, random f_{ca} of 4.6 – 5.4 kHz can reduce the total filter inductance requirement by 40% compared to a fixed f_{ca} of 5 kHz.

B. Component Stress and Harmonic Spectrum

Fig. 12(a) and **12(b)** show the inductor current waveforms of conventional PWM and SSM with f_{ca} variation of 4.6 – 5.4 kHz, respectively, when the same LCL parameters are used. Even though the switching period varies a lot, its impact on the inductor current shape is negligible. Based on this, it can be expected that the power losses of the semiconductors and passives with SSM will still be similar to those with conventional PWM.

Fig. 13 shows the impact of SSM on harmonic spectrum of the grid current if optimized LCL filter designs are employed for each case to satisfy the IEEE519 standard. Damping schemes are not considered. Although the required filter parameters are lower with SSM, significant harmonics are spread even to very low frequency ranges as shown in **Fig. 13 (b)**, which could also be predicted from the spectrums in

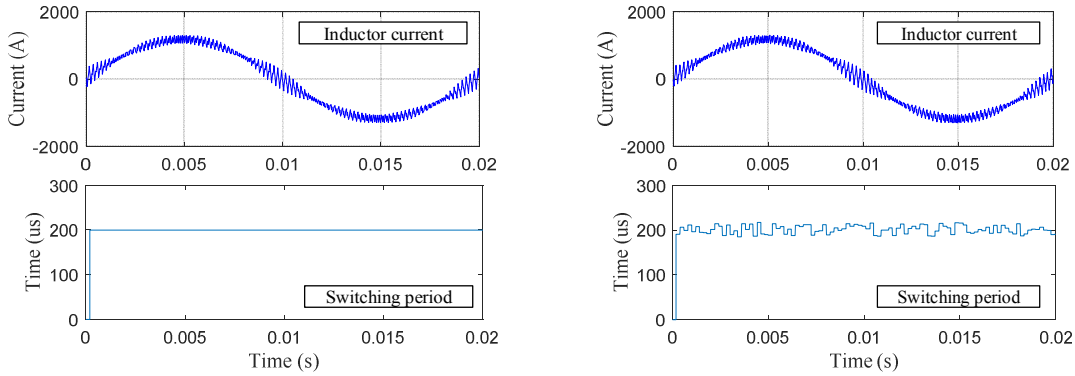

Fig. 12. Comparison of inductor current waveforms for (a) fixed f_{ca} = 5 kHz and (b) random f_{ca} = 4.6…5.4 kHz with conventional pulse positioning. The same LCL filter is used.

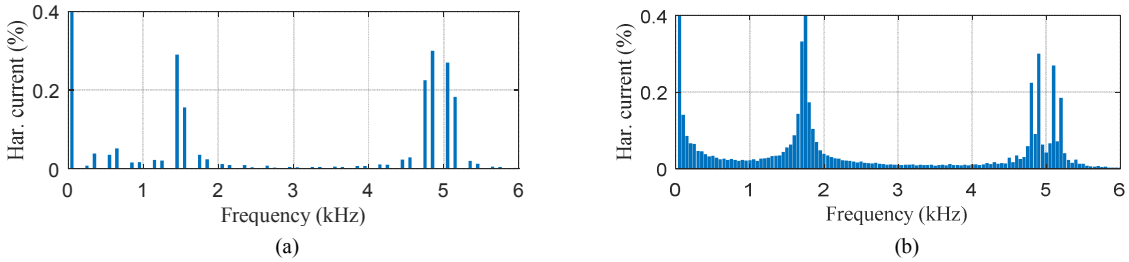

Fig. 13. Comparison of grid-side harmonic current spectrum normalized by the fundamental component between (a) fixed f_{ca} = 5 kHz, k_{res} = 0.3 and (b) random f_{ca} = 4.8…5.2 kHz, k_{res} = 0.35 with conventional pulse positioning. The LCL filter are different and optimized for each case to satisfy IEEE519. No damping is considered.

Fig. 8. Low frequency harmonics which are inside the control bandwidth can be mitigated by the current control. However, the harmonics around the LCL filter resonant frequency potentially cause severe resonances unless proper damping scheme is utilized.

V. Concluding Remarks and Further Works

An LCL filter design methodology for SSM is presented and a comparative analysis between the conventional PWM and SSM is carried out focusing on their impacts on the LCL filter design. It is shown that under the same average f_{ca}, LCL filter parameters required for SSM can be reduced by about 30% with +/- 8% variation of f_{ca}.

As a next step, the impact of SSM on the performance space of the entire system such as efficiency and power density of the grid-tied converter will be investigated, including the side effect of resonance damping of LCL filter.

References

[1] K.-B. Park, F. Kieferndorf, U. Drofenik, S. Pettersson, and F. Canales, "Weight minimization of LCL filters for high power converters: Impact of PWM method on power loss and power density," *IEEE Trans. Ind. Appl.* vol. 53, no. 3, pp. 2282-2296, May/Jun. 2017.

[2] K.-B. Park, "The age of optimization in power electronics," in *Proc. PCIM-Europe*, 2019.

[3] T. Soeiro, K.-B. Park, and F. Canales, "High voltage photovoltaic system implementing Si/SiC-based active neutral-point-clamped converter," in *Proc. IECON*, 2017, pp. 1220-1225.

[4] K.-B. Park, F. Kieferndorf, U. Drofenik, S. Pettersson, and F. Canales, "Optimization of LCL filter with intercell transformer for interleaved voltage source converters," in *Proc. IECON*, 2017, pp. 1375-138.

[5] K. Mainai and R. Oruganti, "Conducted EMI mitigation techniques for switch-mode power conveters: a survey," *IEEE Trans. Power Elec.*, vol. 25, no. 9, pp. 2344-2356, Sep. 2010.

[6] D. Gozanlez *et al*, "Conducted EMI reduction in power converters by means of periodic switching frequency modulation," *IEEE Trans. Power Elec.*, vol. 22, no. 6, pp. 2271-2281, Nov. 2007.

[7] F. Rareschi, R. Rovatti, and G. Setti, "EMI reduction via spread spectrum in DC/DC converters: State of the art, optimization, and tradeoffs," *IEEE Access*, vol. 3, pp. 2857-2874, 2015.

[8] R. Lynn Kirlin, S. Kwok, S. Legowski, and A. M. Trzynadlowski, "Power spectra of a PWM inverter with randomized pulse position," *IEEE Trans. Power Elec.*, vol. 9, no. 5, pp. 463-472, Sep. 1994.

[9] R. Gamoudi, D. E. Chariag, and L. Sbita, "A review of spread-spectrum-based PWM techniques─A novel fast digital implementation," *IEEE Trans. Power Elec.*, vol. 33, no. 12, pp. 10292-10307, Dec. 2018.

[10] K. Lee, G. Shen, W. Yao, and Z. Lu, "Performance characterization of random pulse width modulation algorithm in industrial and commercial adjustable-speed drive," *IEEE Trans. Ind Appl.*, vol. 52, no. 2, pp. 1078-1087, Mar/Apr. 2017.

[11] L. Mathe, F. Lungeanu, D. Sera, P. O. Rasmussen, and J. K. Pedersen, "Spread spectrum modulation by using asymmetric-carrier random PWM," *IEEE Trans. Ind Elec.*, vol. 59, no. 10, pp. 3710-3718, Oct. 2012.

[12] H. Khan, E. Miliani, and K. E. K. Erissi, "Discontinuous random space vector modulation for electric drives: a digital approach," *IEEE Trans. Power Elec.*, vol. 27, no. 12, pp. 4944-4951, Dec. 2012.

[13] C. B. Jacobina, A. M. N. Lima, E. R. C. Silva, and A. M Trzynadlowski, "Current control for induction motor drives using random PWM," *IEEE Trans. Ind. Elec.*, vol. 45, no. 5, pp. 704-712, Oct. 1998.

[14] IEEE Std 519-2014: IEEE recommended practice and requirements for harmonic control in electric power systems, *IEEE Standards Association*, 2014.

[15] K.-B. Park and R. M. Burkart, "Filter hardware optimization of grid-tied converters: LCL vs. LLCL filter," in *Proc. ICRERA*, 2018.

[16] K.-B. Park, "One-phase modulation without DC link control for three-phase rectifier with LCL filter," in *Proc. ICPE*, 2019.